

Instantaneous Hydrolysis of Nerve-Agent Simulants with a Six-Connected Zirconium-Based Metal–Organic Framework**

Su-Young Moon, Yangyang Liu, Joseph T. Hupp,* and Omar K. Farha*

Abstract: A nerve-agent simulant based on a phosphate ester is hydrolyzed using a MOF-based catalyst. Suspensions of MOF-808 (6-connected), a material featuring 6-connected zirconium nodes, display the highest hydrolysis rates among all MOFs that have been reported to date. A plug-flow reactor was also prepared with MOF-808 (6-connected) as the active layer. Deployed in a simple filtration scheme, the reactor displayed high hydrolysis efficiency and reusability.

Many chemical warfare agents (CWAs), such as Sarin (GB) and Soman (GD), have been synthesized and used since World War I.^[1] The mode of action of G-series nerve agents is to rapidly substitute halides/pseudohalides on the nerve agents by forming phosphate ester bonds with acetylcholinesterase, thereby shutting down its activity. The results are accumulation of the neurotransmitter acetylcholine and concomitant derailment of the neural signals responsible for activating muscles, including muscles needed for respiration. The derailment leads to oxygen deprivation and, ultimately, death by asphyxiation.^[1a,2] Although tremendous effort has been invested in developing modified activated carbons or metal oxides for adsorbing or chemically altering this class of CWAs, issues of low capacity and/or slow degradation kinetics have hobbled real-world implementation.^[3] Thus, there is a compelling need to develop new materials that can be incorporated into protective equipment for rapid detoxification of nerve agents or used for the elimination of large stores of CWAs.

The most common method by which phosphate-based nerve agents can be detoxified is hydrolysis of the labile P–X bond (e.g., X = F, CN in the case of G-series nerve agents; Figure 1).^[4] Although phosphate esters can be hydrolyzed

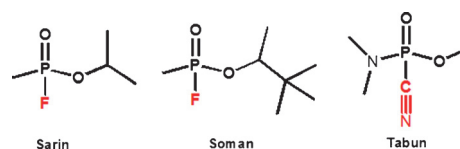


Figure 1. Structural formula of G-series nerve agents.

directly with water,^[4a] the reaction rate is too slow for real-world applications which often require a nearly immediate response. Thus, we have been investigating catalysts for the rapid detoxification of nerve-agent simulants by both hydrolysis and methanolysis. Homogeneous dimers and tetramers of aluminum-porphyrin-based catalysts showed enhanced hydrolysis by catalytic acid activation of the phosphate. A half-life ($t_{1/2}$) of 10 h for the methanolysis reaction was attributed to the favorable positioning of pairs of acidic Al^{III} sites.^[5] Porous organic polymers (POPs) containing Al-porphyrins or La-catecholates moieties demonstrated a nearly seven-fold greater methanolysis rates ($t_{1/2} = 90$ min). Furthermore, the heterogeneous nature of the POPs allowed for facile separation, and thus recyclability, of the catalyst from solution.^[6]

Metal–organic frameworks (MOFs) have been studied as adsorbents and catalysts for removal and detoxification of toxic chemicals due to their exceptional porosity and amenability to modular design.^[7] Along the same lines, we have recently been examining a variety of Zr^{IV}-containing MOFs as catalysts for the hydrolysis of nerve-agent simulants. Owing to their exceptional aqueous stability over a wide range of pH values, Zr-based MOFs are especially attractive candidates as hydrolysis catalysts.^[8] In addition, the versatility of Zr-based nodes as structural elements leads to a tremendous number of high porosity MOFs with diverse organic linkers, topologies, and, potentially, different catalytic activities. Notably, Zr^{IV} is strongly acidic—an attractive feature for activation of coordinated phosphate species. Finally, the nodes of these MOFs which contain zirconium-bridging hydroxo ligands resemble the Zn–OH–Zn active sites of phosphotriesterase enzymes.^[9]

We have previously demonstrated that UiO-66 (12-connected), a nominally 12-connected Zr₆-based MOF, can hydrolyze the nerve-agent simulant dimethyl 4-nitrophenyl phosphate (DMNP) with a $t_{1/2}$ of 50 min at room temperature (Table 1 illustrates the idealized (i.e., defect-free) structure of UiO-66 (12-connected) and associated Zr₆ node).^[9] DMNP, a pesticide containing a phosphate ester bond, is widely used as a nerve-agent simulant owing to its structural similarity to G-series nerve agents, but with the advantage of notably lower toxicity. In a follow up study, we introduced, proximal

[*] Dr. S. Y. Moon,^[4] Dr. Y. Liu,^[4] Prof. J. T. Hupp, Prof. O. K. Farha
 Department of Chemistry
 Northwestern University
 2145 Sheridan Road, Evanston, IL 60208-3113 (USA)
 E-mail: j-hupp@northwestern.edu
 o-farha@northwestern.edu

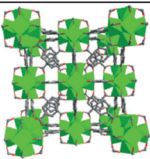
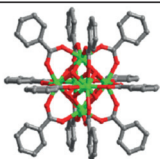
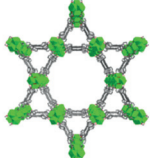
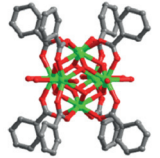
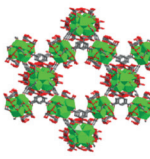
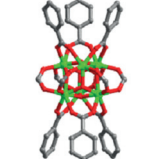
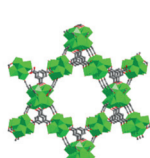
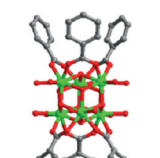
Prof. O. K. Farha
 Department of Chemistry, Faculty of Science, King Abdulaziz
 University
 Jeddah (Saudi Arabia)

[†] These authors contributed equally to this work.

[**] We gratefully acknowledge DTRA for financial support (grant HDTRA-1-10-0023). This work made use of the J. B. Cohen X-Ray Diffraction Facility supported by the MRSEC program of the National Science Foundation (DMR-1121262) at the Materials Research Center of Northwestern University.

Supporting information for this article is available on the WWW under <http://dx.doi.org/10.1002/anie.201502155>.

Table 1: The node connectivity, formula, and structure of UiO-66 (12-connected), NU-1000 (8-connected), and MOF-808 (6-connected) Zr green, O red, C gray, hydrogen atoms are omitted for clarity.

MOF and formula ^[14] (connectivity of the nodes)	Structure	Node
UiO-66 $Zr_6(\mu_3-O)_4(\mu_3-OH)_4(BDC)_6$ (12-connected)		
NU-1000 $Zr_6(\mu_3-O)_4(\mu_3-OH)_4(H_2O)_4(TBAPy)_2$ (8-connected)		
MOF-808-as synthesized $Zr_6(\mu_3-O)_4(\mu_3-OH)_4(HCOO)_6(BTC)_2$		
MOF-808-activated $Zr_6(\mu_3-O)_4(\mu_3-OH)_4(H_2O)_6(BTC)_2$ (6-connected)		

to the Zr_6 node, linker-pendant amines having sufficient basicity to facilitate hydrolysis-related proton-transfer reactions and/or generate hydrolysis-relevant aqueous hydroxide. Regardless of the mechanism, this modification decreases to $t_{1/2}$ of 1 min.^[10]

In defect-free UiO-66 (12-connected), each hexa-zirconium(IV) node is connected to 12 small linkers (i.e. benzene dicarboxylate). The resulting small apertures (ca. 6 Å across) limit catalytic activity to the external surface of the MOF—only about 0.5% of the materials' nodes for the size of MOF particles/crystallites used.^[11] In part to address this limitation, we recently investigated NU-1000 (8-connected) as a phosphate ester hydrolysis catalyst. NU-1000 (8-connected) is based on an 8-connected Zr_6 cluster and tetrapodal 1,3,6,8(*p*-benzoate)pyrene linkers (TBAPy⁴⁻).^[8h,12] Rather than the small aperture of UiO-66 (12-connected), NU-1000 (8-connected) offers notably larger apertures (31 Å diameter channel). The larger apertures facilitate delivery of the nerve-agent simulant to the interior of the MOF, thus enabling a much greater percentage of nodes to act as catalysts for simulant or agent hydrolysis. As anticipated, the half-life for hydrolysis of DMNP with NU-1000 (8-connected) was found to be considerably shorter (15 min) than with unfunctionalized UiO-66 (12-connected) as the catalyst (Table 1). More importantly, each 8-connected Zr_6 node in NU-1000 (8-connected) has four substitutionally labile (i.e., DMNP displaceable) aqua ligands, eliminating the need for structural defects (i.e., missing linkers) to catalyze hydrolysis.^[13] Consistent with rate-limiting substitution of DMNP for water,

intentional dehydration of the nodes of NU-1000 (8-connected) was found to further accelerate the hydrolysis reaction, with $t_{1/2}$ dropping to 1.5 min (Table 2).

Table 2: Comparison of the hydrolysis rate ($t_{1/2}$) of DMNP with various MOFs as well as TOFs for hydrolysis.

MOF	Amount of catalyst [μmol]	$t_{1/2}$ [min]	TOF ^[a] [s ⁻¹]
UiO-66 (12-connected) ^[9]	1.5	35	0.004
UiO-66-NH ₂ (12-connected) ^[10]	1.5	1	0.14
NU-1000 (8-connected) ^[13]	1.5	15	0.009
NU-1000-dehydrated (8-connected) ^[13]	1.5	1.5	0.09
MOF-808 (6-connected)	1.5, 0.7	< 0.5	> 1.4
(this work)	0.3	0.5	1.4

[a] For simplicity, TOF values were calculated at $t_{1/2}$. Slightly larger values are obtained if initial rates are used to calculate TOF.

Since catalytic hydrolysis with NU-1000 (8-connected) is faster than with UiO-66 (12-connected), mainly because of the availability of a much larger number of reactant-accessible, labile water ligands with NU-1000 (8-connected), we hypothesized that Zr_6 -based MOFs with yet lower connectivity might be even more effective as excellent candidates for faster hydrolysis of nerve-agent simulants. To date, Zr_6 MOFs with 12-, 10-, 8-, and 6-connected nodes have been reported. For further investigation, we selected MOF-808 (6-connected).^[8j] Compared with the nodes of all previously studied MOFs, once monodentate modulator ligands (formate ions) are removed, MOF-808 (6-connected)'s hexazirconium(IV) nodes^[15] feature a greater number of ligated water molecules and less linker crowding of Zr^{IV} sites (Table 1). MOF-808 (6-connected) can be readily synthesized from $ZrOCl_2$, benzene-1,3,5-tricarboxylate (BTC), and formic acid in DMF (*N,N'*-dimethylformamide). Each node is connected to six BTC linkers to form 4.8 and 18 Å diameter pores, with remnant formate ions initially occupying six coordination sites. The formate ions can be removed by heating the material in fresh solvent. In their activated (i.e., formate-free) form, each of the nodes of MOF-808 (6-connected) has six water and six hydroxide ligands (Table 1). DRIFTS (diffuse reflectance infrared Fourier transform spectroscopy analysis), NMR spectroscopy and nitrogen adsorption experiments confirmed the activation of MOF-808 (6-connected; Supporting Information, Figure S1–S4).^[12,14] Variable-temperature PXRD (powder X-ray diffraction) measurements show that the MOF retains its crystalline structure up to 250°C (Figure S5). Based on the SEM (scanning electron microscopy) image, the particles size of MOF-808 (6-connected) are approximately 200–350 nm. The DLS (dynamic light scattering) measurement also confirms the presence of 250 nm average particles (Figures S6 and S7).

Figure 2 shows the hydrolysis reaction of nerve-agent simulant DMNP in aqueous buffer solution with MOF-808 (6-connected) as the catalyst. Our previous approach to mon-

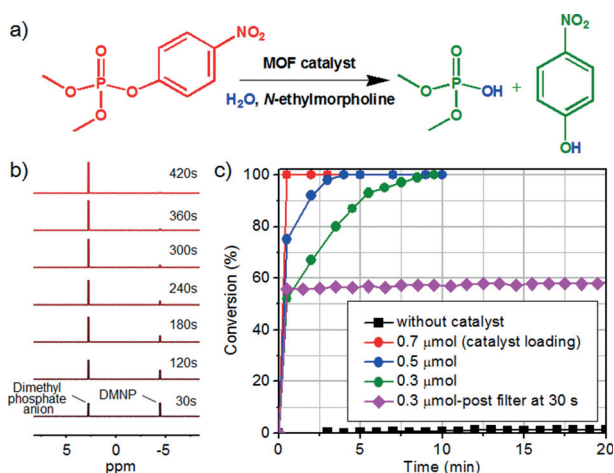


Figure 2. Hydrolysis of DMNP. a) Hydrolysis reaction of DMNP by MOF-based catalysts, b) in situ ^{31}P NMR spectra indicating the progress of hydrolysis of DMNP ($\delta = -4.4$ ppm) to dimethoxy phosphate anion ($\delta = 2.8$ ppm) in the presence of $0.3 \mu\text{mol}$ of MOF-808 (6-connected) at room temperature (reaction conversions at 30 s are obtained by filtering the reaction mixture and measuring the ^{31}P NMR spectrum of the filtrate because the NMR sample requires more than 30 s to prepare), and c) hydrolysis profiles of DMNP in the presence of MOF-808 (6-connected) at different concentrations (circles), after removal of catalyst by filtration (pink diamonds), and without catalyst (black squares).

itoring the heterogeneous reaction kinetics, based on visible-region electronic absorption measurements of product formation proved too slow to capture the kinetics in this case. Consequently, we turned to in situ measurements of ^{31}P NMR spectra. Extents of reaction conversion were calculated by comparing the integrated the ^{31}P peak for DMNP ($\delta = -4.4$ ppm) to that of dimethyl phosphate anion ($\delta = 2.8$ ppm), the hydrolysis product (Figure 2 b,c).

As shown in striking fashion by the data in Figure 2c, the hydrolysis of DMNP in the presence of a catalytic amount of MOF-808 (6-connected) is nearly instantaneous, where the experimental conditions are identical to those we have previously employed (catalyst: $1.5 \mu\text{mol}$ (2.3 mg), simulant: $25 \mu\text{mol}$, at room temperature). Indeed, quantitative conversion of DMNP into the dimethoxy phosphate anion is observed within 30 s, our shortest assessment time. MOF-808 (6-connected) is sufficiently potent as a degradation catalyst that decreasing the catalyst loading from $1.5 \mu\text{mol}$ to $0.7 \mu\text{mol}$ had no discernible effect on the catalysis rate. When the catalyst loading was further lowered to $0.5 \mu\text{mol}$ and $0.3 \mu\text{mol}$, respectively, the hydrolysis reaction was observed to be 75% and 50% complete at 30 s (see Figure 2c and Figure S9–S11). Comparison of the turnover frequency (TOF) of MOF-808 (6-connected) with those of other Zr-based MOFs, including UiO-66-NH₂ (12-connected) and NU-1000-dehydrated (8-connected), indicates that the TOF for MOF-808 (6-connected) is between 10 to 350 times greater (Figure 2c and Table 2).

To determine whether the catalysis is heterogeneous, the reaction mixture was filtered using a 200 nm syringe filter. As can be seen in Figure 2c (pink, diamond trace), no further reaction was observed by in situ ^{31}P NMR (Figure S12) after

filtration. Furthermore, no Zr was detected by inductively coupled plasma-atomic emission analysis (detection limit ca. 1 ppb) of the filtered solution. Control measurements without catalyst revealed negligible hydrolysis (less than 3% after 60 min; Figure S13). We have also investigated Zr-based clusters and $\text{Zr}(\text{OH})_4$ as catalysts for the hydrolysis of DMNP over 60 min, they gave 20% and negligible conversion, respectively.^[13] We conclude, therefore, that the reaction indeed is catalyzed by a solid, and not by a soluble molecule or metal ion. Powder X-ray diffraction (PXRD) measurements were used to examine whether, during the catalyst retains its structure and crystallinity post-catalysis. As seen in Figure S8, the material clearly remains intact, in line with our observations regarding the stability of other Zr-based MOFs under identical reaction conditions.

The fast reaction rate combined with the stability of Zr-based MOFs led us to pursue a simple continuous flow system.^[16] To prepare a MOF plug-flow reactor, MOF-808 (6-connected) was dispersed in water and then loaded onto a commercial polymer membrane by filtration. A 10 mL solution containing $40 \mu\text{L}$ of simulant was then injected through the plug-flow reactor at 0.1 mL min^{-1} ; the filtrate was subjected to ^{31}P NMR spectroscopy every 1 mL to determine extents of conversion for the hydrolysis reaction. As shown in Figure 3, the catalytic hydrolysis reaction (Figure 2a) was

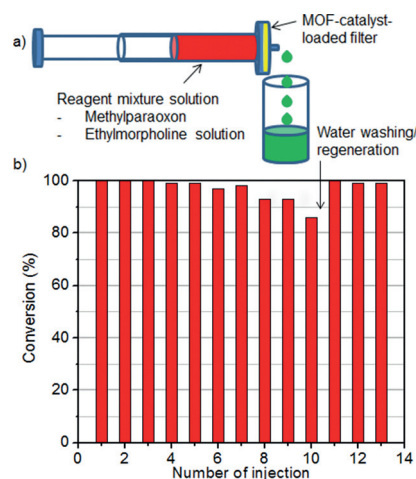


Figure 3. Hydrolysis of DMNP using a MOF plug-flow reactor. a) Schematic representation of the MOF plug-flow reactor, b) percent conversion of DMNP to nitrophenoxide and dimethylphosphate after injection through the plug flow (1 mL/injection); catalyst was washed with water and re-loaded after 10 injections.

quantitative for the first 3 mL, between 99 and 93% for the next six 1 mL increments, and dropping eventually to 87% for the tenth mL. After 10 mL the MOF catalyst was isolated from the polymer membrane, washed with water, and loaded back onto the membrane. The reloaded material quantitatively converted (ca. 99%) the 11th mL and nearly quantitatively converted (ca. 99%) the 12th and 13th mL. Together these experiments illustrate that the catalyst can readily be regenerated.

In conclusion, MOF-808 (6-connected) shows extraordinary catalytic activity for the hydrolysis of the nerve-agent

simulant DMNP. Indeed, the observed TOF for MOF-808 (6-connected) exceeds those of Zr₆-based MOFs by up to 350-fold. We find that MOF-808 (6-connected) can be effectively used as the catalytic element of a simple plug-flow reactor; under conditions of continuous flow it yields high reaction conversion and is readily reusable. We believe that the number of water molecules ligated to the Zr₆-node (inversely proportional to the number of connections to the node), as well as the relative accessibility of nodes to reactant molecules, are important factors in modulating the catalytic rate. However, we also believe other factors, such as ligand acidity and/or rates of aqua ligand exchange with the solvent, contribute to the observed differences. We are currently investigating some of these factors by measuring pK_a values of Zr₆ nodes featuring different connectivities. We hope to report on our findings in the near future.^[17]

Experimental Section

All reagents were purchased from commercial sources and used without further purification. MOF-808 (6-connected) and DMNP were synthesized as reported previously.^[5a,8j]

Hydrolysis profiles were recorded by in situ ³¹P NMR measurement at room temperature. A MOF-808 (6-connected) catalyst (FW: 1551, 1.1 mg, 0.7 μmol; 0.8 mg, 0.5 μmol; 0.5 mg, 0.3 μmol) was loaded into a 1.5 dram vial and 0.4 M *N*-ethylmorpholine solution (1 mL; 0.05 mL *N*-ethylmorpholine, 0.9 mL DI water/0.1 mL D₂O) was added and then stirred for 15 min to disperse homogeneously. DMNP (4 μL; 25 μmol was added to mixture solution and swirled for 10 s. The reaction mixture was then transferred to an NMR tube and the spectrum was immediately measured; the first data point was collected 120 s after the start of the reaction. The progress of the reaction was monitored with 1 min increments for 1 h (number of scans = 16, delay time = 28 s). The solvent was 10% D₂O/H₂O. To measure reaction conversions at 30 s, a reaction mixture was prepared under identical conditions and filtered using a 200 nm syringe filter at 30 s, thereby stopping the reaction and permitting the degree of completion to be assessed by ³¹P NMR. Background reactivity was evaluated under identical conditions, apart from the absence of catalyst, and monitored by in situ ³¹P NMR. To confirm the heterogeneous nature of the catalyst, the reaction mixture with 0.3 μmol of MOF-808 (6-connected) was passed through a syringe filter (200 nm pores) at 30 s; the composition of the filtrate was then monitored for 1 h by ³¹P NMR spectroscopy.

Keywords: heterogeneous catalysis · hydrolysis · metal-organic frameworks · MOF plug-flow reactor · nerve agents

How to cite: *Angew. Chem. Int. Ed.* **2015**, *54*, 6795–6799
Angew. Chem. **2015**, *127*, 6899–6903

[1] a) A. Watson, D. Opresko, R. Young, V. Hauschild, J. King, K. Bakshi in *Handbook of Toxicology of Chemical Warfare Agents* (Ed.: R. C. Gupta), Academic Press, San Diego, **2009**, pp. 43–67; b) Y. C. Yang, J. A. Baker, J. R. Ward, *Chem. Rev.* **1992**, *92*, 1729–1743; c) J. Bajgar, J. Fusek, J. Kassa, K. Kuca, D. Jun in *Handbook of Toxicology of Chemical Warfare Agents* (Ed.: R. C. Gupta), Academic Press, San Diego, **2009**, pp. 17–24; d) N. H. Johnson, J. C. Larsen, E. Meek in *Handbook of Toxicology of Chemical Warfare Agents* (Ed.: R. C. Gupta), Academic Press, San Diego, **2009**, pp. 7–16; e) T. Okumura, K. Taki, K. Suzuki, T. Satoh in *Handbook of Toxicology of Chemical Warfare Agents* (Ed.: R. C. Gupta), Academic Press, San Diego, **2009**, pp. 25–

32; f) M. Enserink, *Science* **2013**, *341*, 1050–1051; g) R. Pita, J. Domingo, *Toxics* **2014**, *2*, 391–402.
[2] A. N. Bigley, F. M. Raushel, *Biochim. Biophys. Acta Proteins Proteomics* **2013**, *1834*, 443–453.
[3] a) G. W. Peterson, J. A. Rossin, *Ind. Eng. Chem. Res.* **2011**, *51*, 2675–2681; b) J. A. Rossin, R. W. Morrison, *Carbon* **1991**, *29*, 887–892; c) A. H. Maxwell, J. A. Rossin, *Carbon* **2010**, *48*, 2634–2643; d) G. W. Wagner, G. W. Peterson, J. J. Mahle, *Ind. Eng. Chem. Res.* **2012**, *51*, 3598–3603; e) T. J. Badosz, M. Laskoski, J. Mahle, G. Mogilevsky, G. W. Peterson, J. A. Rossin, G. W. Wagner, *J. Phys. Chem. C* **2012**, *116*, 11606–11614.
[4] a) G. Lunn, E. Sansone, *Appl. Biochem. Biotechnol.* **1994**, *49*, 165–172; b) M. K. Kinnan, W. R. Creasy, L. B. Fullmer, H. L. Schreuder-Gibson, M. Nyman, *Eur. J. Inorg. Chem.* **2014**, 2361–2367.
[5] a) R. K. Totten, P. Ryan, B. Kang, S. J. Lee, L. J. Broadbelt, R. Q. Snurr, J. T. Hupp, S. T. Nguyen, *Chem. Commun.* **2012**, *48*, 4178–4180; b) B. Kang, J. W. Kurutz, K.-T. Youm, R. K. Totten, J. T. Hupp, S. T. Nguyen, *Chem. Sci.* **2012**, *3*, 1938–1944.
[6] a) R. K. Totten, Y.-S. Kim, M. H. Weston, O. K. Farha, J. T. Hupp, S. T. Nguyen, *J. Am. Chem. Soc.* **2013**, *135*, 11720–11723; b) R. K. Totten, M. H. Weston, J. K. Park, O. K. Farha, J. T. Hupp, S. T. Nguyen, *ACS Catal.* **2013**, *3*, 1454–1459.
[7] a) J. B. DeCoste, G. W. Peterson, *Chem. Rev.* **2014**, *114*, 5695–5727; b) E. Barea, C. Montoro, J. A. R. Navarro, *Chem. Soc. Rev.* **2014**, *43*, 5419–5430.
[8] a) J. H. Cavka, S. Jakobsen, U. Olsbye, N. Guillou, C. Lamberti, S. Bordiga, K. P. Lillerud, *J. Am. Chem. Soc.* **2008**, *130*, 13850–13851; b) C. Wang, J.-L. Wang, W. Lin, *J. Am. Chem. Soc.* **2012**, *134*, 19895–19908; c) C. Wang, Z. Xie, K. E. deKrafft, W. Lin, *J. Am. Chem. Soc.* **2011**, *133*, 13445–13454; d) H.-L. Jiang, D. Feng, T.-F. Liu, J.-R. Li, H.-C. Zhou, *J. Am. Chem. Soc.* **2012**, *134*, 14690–14693; e) D. Feng, Z.-Y. Gu, J.-R. Li, H.-L. Jiang, Z. Wei, H.-C. Zhou, *Angew. Chem. Int. Ed.* **2012**, *51*, 10307–10310; *Angew. Chem.* **2012**, *124*, 10453–10456; f) W. Morris, B. Voloskiy, S. Demir, F. Gándara, P. L. McGrier, H. Furukawa, D. Cascio, J. F. Stoddart, O. M. Yaghi, *Inorg. Chem.* **2012**, *51*, 6443–6445; g) D. Feng, W.-C. Chung, Z. Wei, Z.-Y. Gu, H.-L. Jiang, Y.-P. Chen, D. J. Darensbourg, H.-C. Zhou, *J. Am. Chem. Soc.* **2013**, *135*, 17105–17110; h) J. E. Mondloch, W. Bury, D. Fairen-Jimenez, S. Kwon, E. J. DeMarco, M. H. Weston, A. A. Sarjeant, S. T. Nguyen, P. C. Stair, R. Q. Snurr, O. K. Farha, J. T. Hupp, *J. Am. Chem. Soc.* **2013**, *135*, 10294–10297; i) H. Furukawa, F. Gándara, Y.-B. Zhang, J. Jiang, W. L. Queen, M. R. Hudson, O. M. Yaghi, *J. Am. Chem. Soc.* **2014**, *136*, 4369–4381; j) M. Kim, J. F. Cahill, H. Fei, K. A. Prather, S. M. Cohen, *J. Am. Chem. Soc.* **2012**, *134*, 18082–18088; k) S. Pullen, H. Fei, A. Orthaber, S. M. Cohen, S. Ott, *J. Am. Chem. Soc.* **2013**, *135*, 16997–17003; l) H. Fei, S. M. Cohen, *Chem. Commun.* **2014**, *50*, 4810–4812; m) M. Kim, S. M. Cohen, *CrystEngComm* **2012**, *14*, 4096–4104.
[9] M. J. Katz, J. E. Mondloch, R. K. Totten, J. K. Park, S. T. Nguyen, O. K. Farha, J. T. Hupp, *Angew. Chem. Int. Ed.* **2014**, *53*, 497–501; *Angew. Chem.* **2014**, *126*, 507–511.
[10] M. J. Katz, S.-Y. Moon, J. E. Mondloch, M. H. Beyzavi, C. J. Stephenson, J. T. Hupp, O. K. Farha, *Chem. Sci.* **2015**, *6*, 2286–2291.
[11] a) P. Ghosh, Y. J. Colon, R. Q. Snurr, *Chem. Commun.* **2014**, *50*, 11329–11331; b) F. Vermoortele, B. Bueken, G. Le Bars, B. Van de Voorde, M. Vandichel, K. Houthoofd, A. Vimont, M. Daturi, M. Waroquier, V. Van Speybroeck, C. Kirschhock, D. E. De Vos, *J. Am. Chem. Soc.* **2013**, *135*, 11465–11468.
[12] N. Planas, J. E. Mondloch, S. Tussupbayev, J. Borycz, L. Gagliardi, J. T. Hupp, O. K. Farha, C. J. Cramer, *J. Phys. Chem. Lett.* **2014**, *5*, 3716–3723.
[13] J. E. Mondloch, M. J. Katz, W. C. Isley III, P. Ghosh, P. Liao, W. Bury, G. W. Wagner, M. G. Hall, J. B. DeCoste, G. W. Peterson,

- R. Q. Snurr, C. J. Cramer, J. T. Hupp, O. K. Farha, *Nat. Mater.* **2015**, *14*, 512–516.
- [14] The proton topology of MOF-808 (6-connected) is still under investigation and a thorough study similar to the study conducted by Planas et al. (see Ref. [12]) on NU-1000 (8-connected) is still needed to determine the order of water and hydrolysis molecules on the node.
- [15] D. Feng, K. Wang, J. Su, T.-F. Liu, J. Park, Z. Wei, M. Bosch, A. Yakovenko, X. Zou, H.-C. Zhou, *Angew. Chem. Int. Ed.* **2015**, *54*, 149–154; *Angew. Chem.* **2015**, *127*, 151–156.
- [16] I. F. J. Vankelecom, *Chem. Rev.* **2002**, *102*, 3779–3810.
- [17] While this article was in press we learned of a related study: E. López-Maya, C. Montoro, L. M. Rodríguez-Albelo, S. D. Aznar Cervantes, A. A. Lozano-Pérez, J. L. Cenís, E. Barea, J. A. R. Navarro *Angew. Chem. Int. Ed.* **2015**, *54*, 6790–6794; *Angew. Chem.* **2015**, *127*, 6894–6898.

Received: March 6, 2015

Published online: May 7, 2015